THE ASTRONOMICAL JOURNAL, 121:2540–2548, 2001 May
© 2001. The American Astronomical Society. All rights reserved. Printed in U.S.A.

FABRY-PÉROT Hα OBSERVATIONS OF THE BARRED SPIRAL NGC 3367

J. ANTONIO GARCÍA-BARRETO AND M. ROSADO
Instituto de Astronomía, Universidad Nacional Autónoma de México (UNAM), Apartado Postal 70-264, México D.F. 04510, México
Received 2000 October 11; accepted 2001 January 18

ABSTRACT

We report the gross properties of the velocity field of the barred spiral galaxy NGC 3367. We obtained the following values: the inclination with respect to the plane of the sky, $i = 30$; the position angle (P.A.) of the receding semimajor axis, P.A. = 51°; and the systemic velocity, $V_{sys} = 3032$ km s^{-1}. Large velocity dispersions are observed of up to 120 km s^{-1} in the nuclear region and of up to 70 km s^{-1} near the eastern bright sources just beyond the edge of the stellar bar, where three spiral arms seem to start, and in the western bright sources at about 10 kpc. Deviations from normal circular velocities are observed from the whole disk but mainly from the semicircle formed by the string of southwestern Hα sources. An estimate of the dynamical mass is $M_{dyn} = 2 \times 10^{11}\ M_{\odot}$.

Key words: galaxies: individual (NGC 3367) — galaxies: kinematics and dynamics — galaxies: structure

1. INTRODUCTION

NGC 3367 is an SBc barred spiral galaxy that is considered to be isolated at a distance of 43.6 Mpc behind the Leo Spur group of galaxies (i.e., using $H_0 = 75$ km s^{-1} Mpc^{-1}; Tully 1988), with a distant neighbor, NGC 3419, at 900 ± 100 kpc away. At a distance of 43.6 Mpc, 1″ corresponds to 210 pc. Its optical appearance in the broadband filter I ($\lambda = 8040$ Å from García-Barreto, Franco, & Carrillo 1996a; García-Barreto et al. 1996b) is shown in Figure 1; it suggests a galaxy almost face-on, but compilation values from the published papers indicate that its inclination with respect to the plane of the sky is not well determined. Although the weak optical emission originates from an almost axisymmetric disk, the bright emission shows an asymmetry such that the southwestern region looks symmetric, but not the northeastern region. The stellar bar has a radius of only 16″ (3.3 kpc), oriented at P.A. 63° ± 5°, and there is an optical structure consisting of several Hα knots and resembling a "bow shock" at a radius of about 10 kpc from the nucleus, from southeast to northwest (García-Barreto et al. 1996a, 1996b). Very Large Array (VLA) observations at an angular resolution of 4″.5 at 1.46 GHz show radio continuum emission from two lobes extending to at least 6 kpc, straddling the nucleus, most likely off the plane, as well as weaker emission from the disk (García-Barreto et al. 1998). Soft X-ray emission has been reported by Giogia et al. 1990. Single-dish 21 cm H I observations indicate a systemic velocity of $v = 3035 \pm 8$ km s^{-1} and a total hydrogen mass of $M(\mathrm{H\,I}) = 5 \pm 2 \times 10^9\ M_{\odot}$ (Helou et al. 1981; Huchtmeier & Seiradakis 1985; Mirabel & Sanders 1988; Staveley-Smith & Davies 1988). The optical systemic velocity is $v = 2850 \pm 50$ km s^{-1} (Véron-Cetty & Véron 1986; de Vaucouleurs et al. 1991; Véron, Gonçalves, & Véron-Cetty 1997; Ho, Filippenko, & Sargent 1995; 1997).

In this paper, we present new Fabry-Pérot Hα observations of NGC 3367 carried out with the PUMA equipment attached to the San Pedro Mártir 2.1 m optical telescope in Baja California, México. The velocity field thus obtained indicates that differential rotation appears to dominate. Departures from near circular rotation are clear from the central region and also from the outer bright semicircle to the southwest. The fitted rotation curve shows a slow rise and a flat part. Section 2 presents the observations and calibration, § 3 presents the data reduction and analysis, § 4 presents the velocity field, § 5 presents the discussion, and finally § 6 presents the conclusions.

2. OBSERVATIONS AND CALIBRATION

The two-dimensional velocity field for the ionized gas in NGC 3367 was obtained by using the UNAM scanning Fabry-Pérot (FP) interferometer PUMA on 1999 February 8 and 9. This instrument is currently in use at the f/7.9 Ritchey-Chrétien focus of the 2.1 m telescope at the Observatorio Astronómico Nacional at San Pedro Mártir, Baja California, México.

The PUMA setup consists of a scanning Fabry-Pérot interferometer, a focal reducer of 2:1, which brings the initial focal ratio from f/7.9 to f/3.95, a f/3.95 camera, a filter wheel, a calibration system, and a Tektronix CCD detector of 1024 × 1024 pixels (Rosado et al. 1995). Since NGC 3367 has angular dimensions less than 3′, we used only a central region of the CCD of 512 × 512 pixels. In this way, we observed a field of view of 5′ × 5′, with a pixel size of 0″.6 ± 0″.01.

To obtain FP data cubes of NGC 3367, we used an interference filter with a central wavelength of 6620 Å and a narrow band (30 Å) in order to isolate the redshifted Hα emission of this galaxy. The gap between the plates of the FP interferometer, with an interference on the order of 330 at Hα, was scanned over a free spectral range, and a total of 48 interference channels (each 120 s of integration time) were obtained, with a velocity increment of 19 km s^{-1}. Thus, the data cubes are 512 × 512 × 48.

Calibration cubes were obtained before and after the cubes corresponding to NGC 3367. The line at 6598.95 Å of a neon lamp was used for wavelength calibration.

The raw data were calibrated in wavelength using the specialized software CIGALE, developed at the Marseille Observatory (Le Coarer et al. 1993), and object cubes were produced, consisting of 48 velocity maps of 512 × 512 with a final image scale of 0″.6 pixel^{-1} and a spectral sampling of 19 km s^{-1}. No attempt was made for absolute calibration of the Hα emission.

3. DATA REDUCTION AND ANALYSIS

The cube was exported from CIGALE to the AIPS package in a FITS format in order to continue with the data analysis. Preliminary inspection of the emission at different

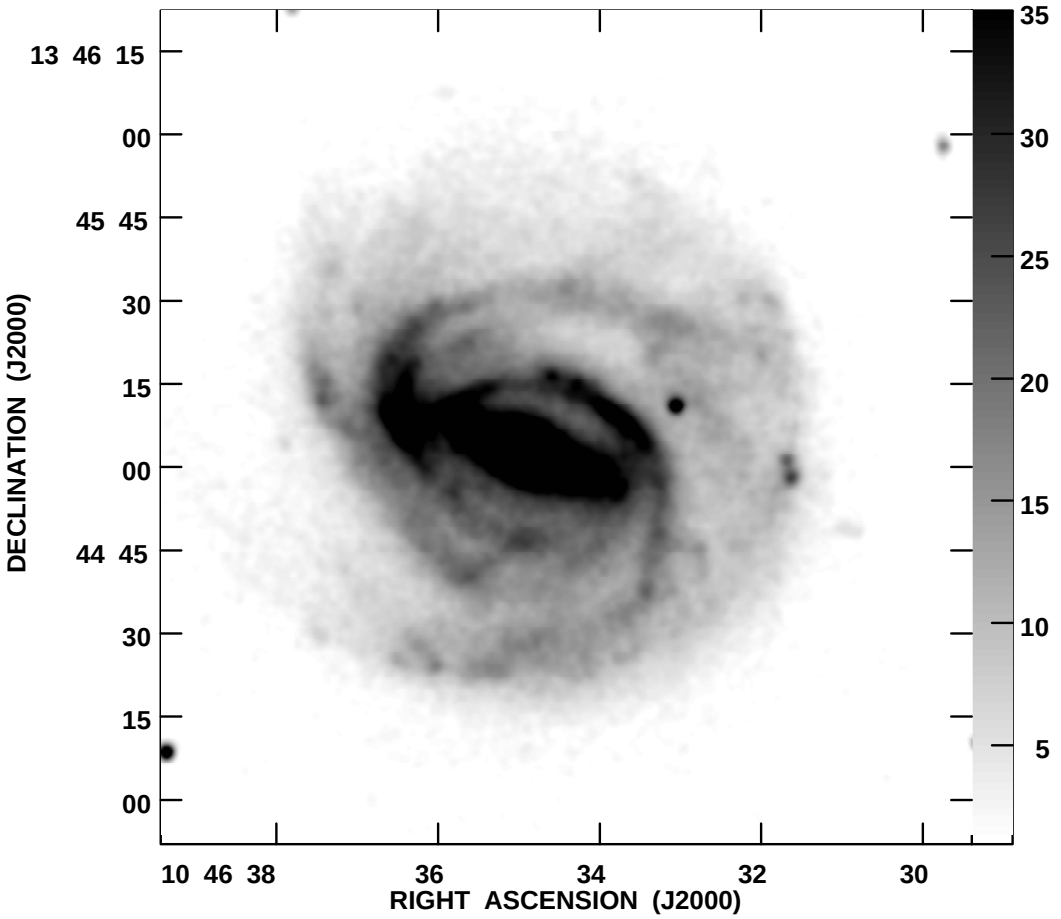


FIG. 1.—Optical continuum emission from NGC 3367 in the broadband filter I (λ8040 Å), convolved to an output beam FWHM of 1.″5 (dictated from the seeing conditions, according to García-Barreto et al. 1996b). Gray scale is proportional to the peak brightness distribution in arbitrary units.

velocities showed that a bright southwestern star was elongated in a P.A. of 13°. Having no idea whether it was a double star from our observations or from POSS plates or anything arising from an instrumental effect that one could possibly correct for, it was decided to convolve the 48 planes to an output Gaussian beam of 6.″5 × 4.″1 at P.A. 13° with the task CONVL, based on the fits on the southwestern star. With this beam, the experiment was aimed mainly at the velocity field with a medium angular resolution. This, as mentioned later, turned out to be crucial in preventing us from studing the kinematics of the most central region of the galaxy. For the best continuum image, it was decided to align all the image planes as well as possible. For this purpose, careful position determinations using IMSTAT and IMFIT were used in AIPS for the nuclear position and a bright southwestern star in the field. It was decided to obtain shifts with respect to plane 25, which showed the maximum brightness (in arbitrary units) for both the nuclear region and the star. Shifts less than 3.6 pixels in R.A. and 0.9 pixels in decl. were found for the nuclear region, and less than 1.5 pixels in R.A. and 0.63 pixels in decl. were found in the southwestern star. Individual planes were corrected for the corresponding shifts found using the program LGEOM in AIPS. A continuum offset was determined from regions outside galaxy emission and corrected for in each plane with the program COMB. In order to obtain a continuum emission from the cube to be subtracted from each plane, the data were displayed for every velocity channel, and it was visually decided which channels had no emission. Finally, channels 2–13 and 37–48 were chosen. First, an image was produced from channels 2–13, using the program SQASH, and then another image using the channels 37–48. Both images were then averaged using the program COMB in order to obtain a final continuum image. This continuum image was subtracted from the cube. Finally, the program MOMNT in AIPS was used to obtain the moments 0 (integrated intensity), 1 (velocity), and 2 (velocity dispersion), after smoothing the data with a boxcar of size 5 and 7 in velocity and space coordinates. After careful inspection of the results using different cutoff values for flux and intensity, it was decided to allow only data using fluxes and intensities above values that guarantee the determination of a velocity field where weak, but above noise level, emission was detected. Figure 2 shows the moment 0, or total integrated intensity, map of the Hα emission. The map is similar to the previous map obtained with a direct image camera taken at the same observatory (García-Barreto et al. 1996a, 1996b, 1998). Figure 3 shows the channel maps, with the heliocentric radial velocities indicated, corresponding to channels 18–33. Figure 4 shows the isovelocity contours plotted on a gray-scale representation of the same Hα distribution shown in Figure 2. Figure 5 shows the velocity dispersion, and Figure 6 shows the residual velocity field (observed minus model).

The program GAL in AIPS was used in order to get the rotation curve. The observed velocity at a given radius is

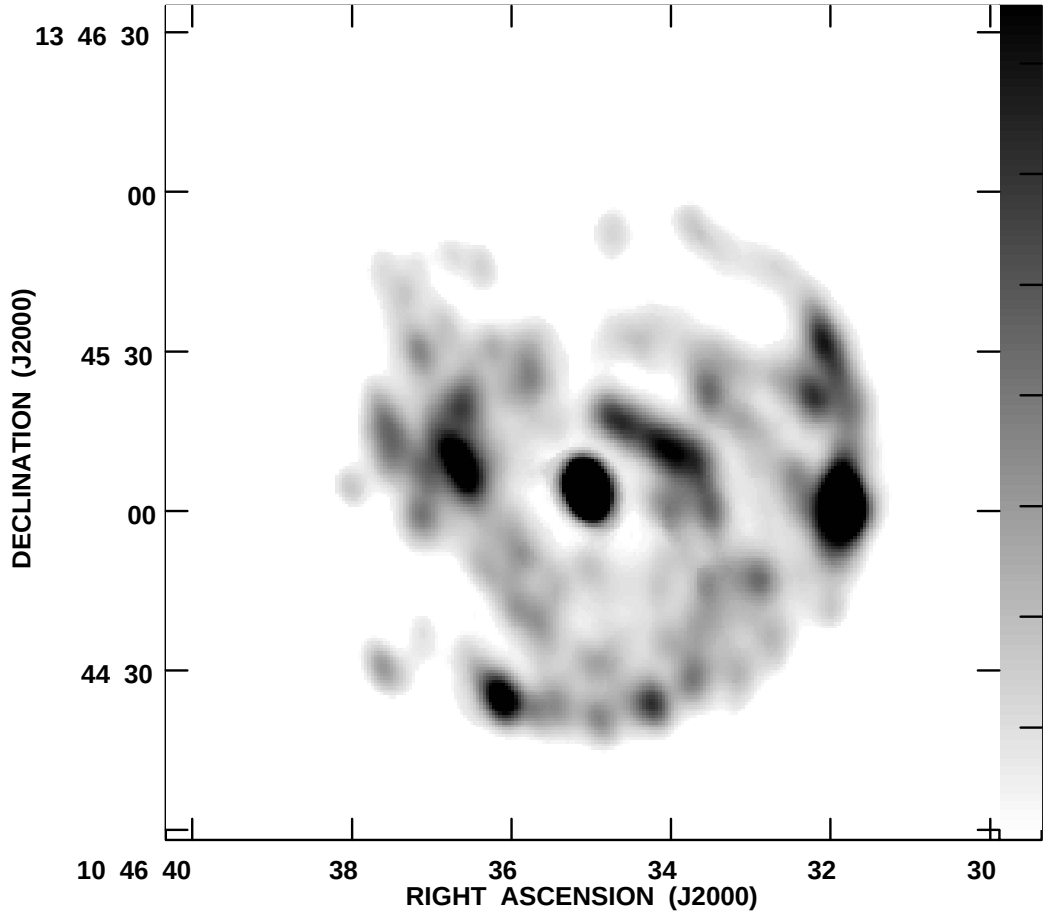


FIG. 2.—Integrated intensity of Hα emission moment 0 map in NGC 3367. Contours and gray scale are proportional to the peak brightness distribution in arbitrary units.

given by the expression

$$V_{\rm obs} = V_{\rm sys} + V_\theta(R, \theta) \sin i \cos \theta + V_R(R, \theta) \sin i \sin \theta + V_z(R, \theta) \cos i ,$$

where i is the inclination of the disk with respect to the plane of the sky, θ is the azimuthal angle in the plane of the galaxy, $V_\theta(R)$ is the azimuthal velocity at a radius R, $V_R(R)$ is the radial velocity component at a radius R, $V_z(R)$ is the vertical velocity component at a radius R, and $V_{\rm sys}$ is the systemic velocity of the galaxy (Mihalas & Binney 1981). As a first approximation, the program GAL assumes that the gas is in near circular orbits in a plane; that is, it considers the $V_R(R)$ and $V_z(R)$ velocity components equal to zero. This assumption will be not valid in the case of NGC 3367, as is seen below. The orientation in space of a galaxy is described, in general, by four parameters: the position of the center (x and y), the position angle of the receding semi-major axis (P.A.), and the inclination of the plane (i). Other parameters involve the systemic velocity ($V_{\rm sys}$), the maximum rotation velocity ($V_{\rm max}$), and the radius at which the maximum rotation velocity occurs ($R_{\rm max}$; van Moorsel & Wells 1985). Our first attempt was to allow all parameters, x, y, P.A., i, $V_{\rm sys}$, $V_{\rm max}$, and $R_{\rm max}$, to vary, using both the receding and approaching sides. The fitted values for the different parameters were $x = 10^{\rm h}46^{\rm m}35\overset{\rm s}{.}04$, $y = +13°45'06\overset{''}{.}4$, P.A. $= 52°$, $i = 30$, $V_{\rm sys} = 3034$ km s^{-1}, $V_{\rm max} = 208$ km s^{-1}, and $R_{\rm max} = 49''$. The fitted values for the x and y position corresponded to the kinematical center $\sim 0\overset{''}{.}5$ west in R.A. and $\sim 2\overset{''}{.}1$ north in decl. from the center of surface brightness maximum. Varying the values of some parameters, while holding others fixed, we tried to get the best rotation curve.

4. VELOCITY FIELD

It is not advisable to make an elaborate many-parameter fit to the rotation curve; however, the fitting of the orientation parameters is by far the most important task (van Moorsel & Wells 1985). It was noticed that the kinematical center fitted with all parameters free to vary was off by about $-0\overset{''}{.}5$ in R.A. and $+2\overset{''}{.}3$ in decl. from the center of the brightness distribution. At this point, it is necessary to mention that the coordinate grid of the cube was anchored in such a way as to make the maximum Hα brightness distribution and the peak of emission in the high-resolution VLA 3.6 cm radio continuum from the central region (which we think corresponds to the nucleus; García-Barreto & Rudnick 2001) coincide. We decided to fix the position of the x and y coordinates to the maximum of the integrated intensity distribution, that is, at $\alpha = 10^{\rm h}46^{\rm m}35\overset{''}{.}06$, $\delta = +13°45'04\overset{''}{.}1$. We ran the program fixing different parameters and fitting others as listed in Table 2.

Average values of $V_{\rm max}$ for small diameter Sc galaxies with high-inclination angles are between 150 and 200 km s^{-1} (Rubin et al. 1985; Rubin, Waterman, & Kenney 1999). Since the value of the inclination i has been reported in the

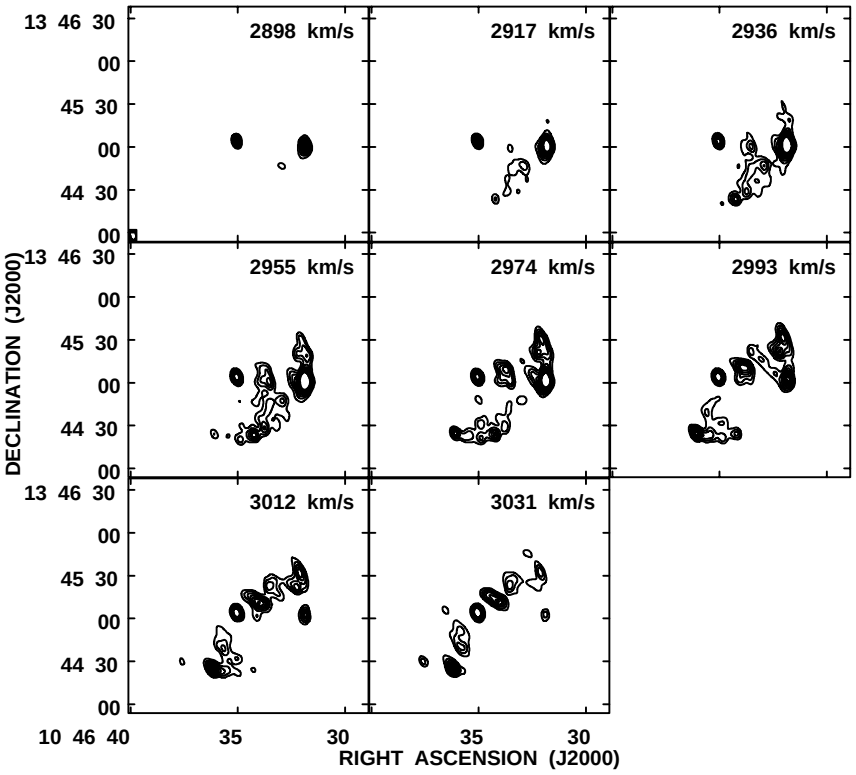


Fig. 3*a*

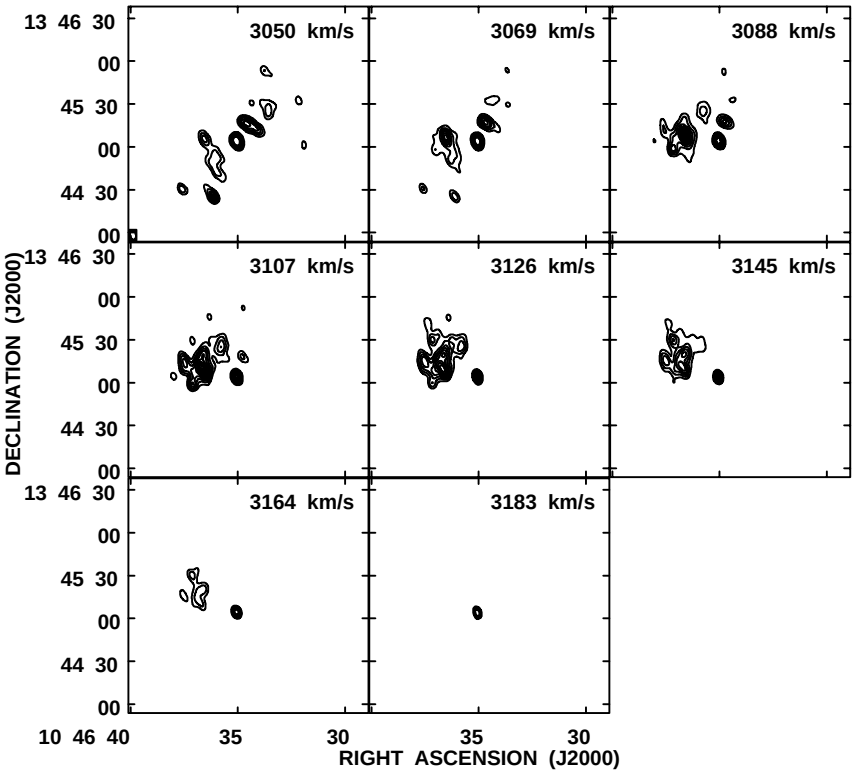


Fig. 3*b*

FIG. 3.—Individual channel maps of intensity distribution in NGC 3367. Contours are proportional to peak brightness in arbitrary units. Velocities in the top right corner are heliocentric velocities and correspond to a channel separation of 19 km s^{-1}. These maps correspond to channels 18–25 in (*a*) and channels 26–33 in (*b*).

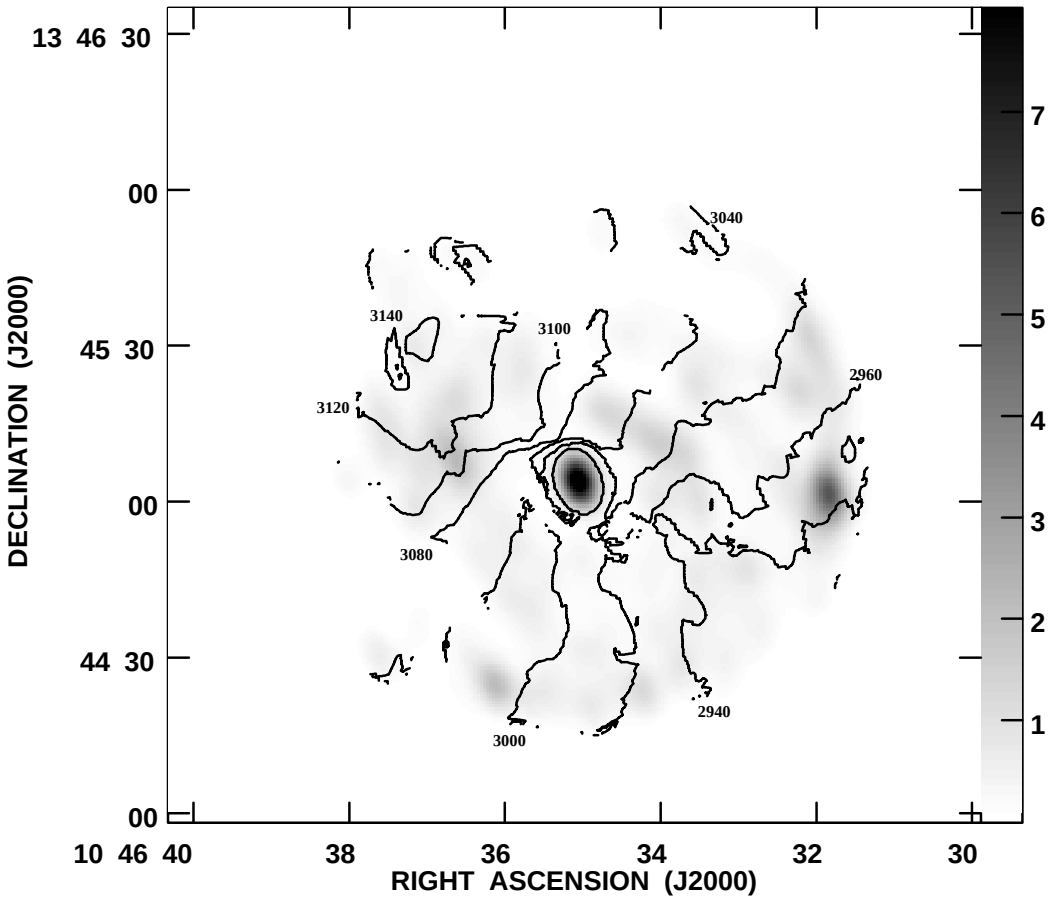


FIG. 4.—Isovelocity contours (moment 1) superposed on the total integrated intensity (moment 0) map. Kinematic receding semimajor axis was found to be at P.A. = 51°. Velocities shown are 2940, 2960, 3000, 3040, 3080, 3100, 3120, and 3140 km s^{-1}; V_{sys} = 3032 km s^{-1}.

range of 6°–37°, a search for reported values of the inclination of NGC 3367 followed. Table 1 lists inclination angles found in the literature for NGC 3367 and the particular method used.

In general, determination of the inclination of a galaxy has been done in any of three methods: (1) multiparametered fits to detailed high-resolution radio synthesis or Fabry-Pérot maps; (2) an axial ratio corrected for spiral arm structure; and (3) an axial ratio according to the formula (Hubble 1926; Mihalas & Binney 1981)

$$\cos^2 i = [(b/a)^2 - (b_i/a_i)^2]/[1 - (b_i/a_i)^2] ,$$

where a and b are the apparent semimajor and semiminor axes of a galaxy, and a_i and b_i are the intrinsic semimajor and semiminor axes. In general, for a flattened spheroid the intrinsic axial ratio is taken to be 0.2 (Holmberg 1958).

As stated by Aaronson, Mould, & Huchra (1980) method 1 is the best method for measuring sin i, since it is the only one that actually measures the inclination of the rotating gas and is based on quantitative analysis of kinematic structure, except for kinematic departures from differential rotation, such as H I warps (Bosma 1981). Aaronson et al. (1980) found that inclinations determined from axial ratios taken from the Second Reference Catalog of Bright Galaxies were too face-on by about 3°.

To evaluate our inclination and position angle of the receding semimajor axis values, we looked at the residual velocity field (observations minus model) for the different values of the inclination, namely, $i = 20°$, $i = 25°$, and $i = 30°$, and two values for the position angle of the receding semimajor axis, P.A. = 46° and 51°. The rotation curve was slightly modified but mainly only on the velocity scale. We did run the program using only $\pm 60°$ from the P.A. of the line of nodes of both the receding and approaching sides in order to look for asymmetry deviations, but we did not find any. Finally, we also tried leaving out the central 10″. As a result, the residual velocity field with the least asymmetries was the one using an inclination of $i = 30°$. Values for inclination and maximum rotation velocity are listed in Table 2.

The maximum velocity is in agreement with the estimated maximum velocity value obtained from H I measurements, $V_{max} = (1/2)\Delta V^{50}_{HI}/\sin i$, since for NGC 3367, $\Delta V^{50}_{HI} = 206$ km s^{-1} (Huchtmeier & Seiradakis 1985). It is smaller, though, by about 50 km s^{-1} from the estimated value, if using the width of the H I line at 20% (ΔV^{20}_{HI}).

The final rotation curve, assuming as usual azimuthal symmetry and zero vertical and radial components of the velocity vector, is shown in Figure 7. This rotation curve can be fitted as a first approximation by a Brandt curve (Brandt 1960), with $V_{max} = 210$ km s^{-1} at $R_{max} = 52''$ (11 kpc). An estimate of the dynamical mass using V_{max} and R_{max} has been obtained. Radio interferometric detection of atomic hydrogen (from larger radii than the maximum dis-

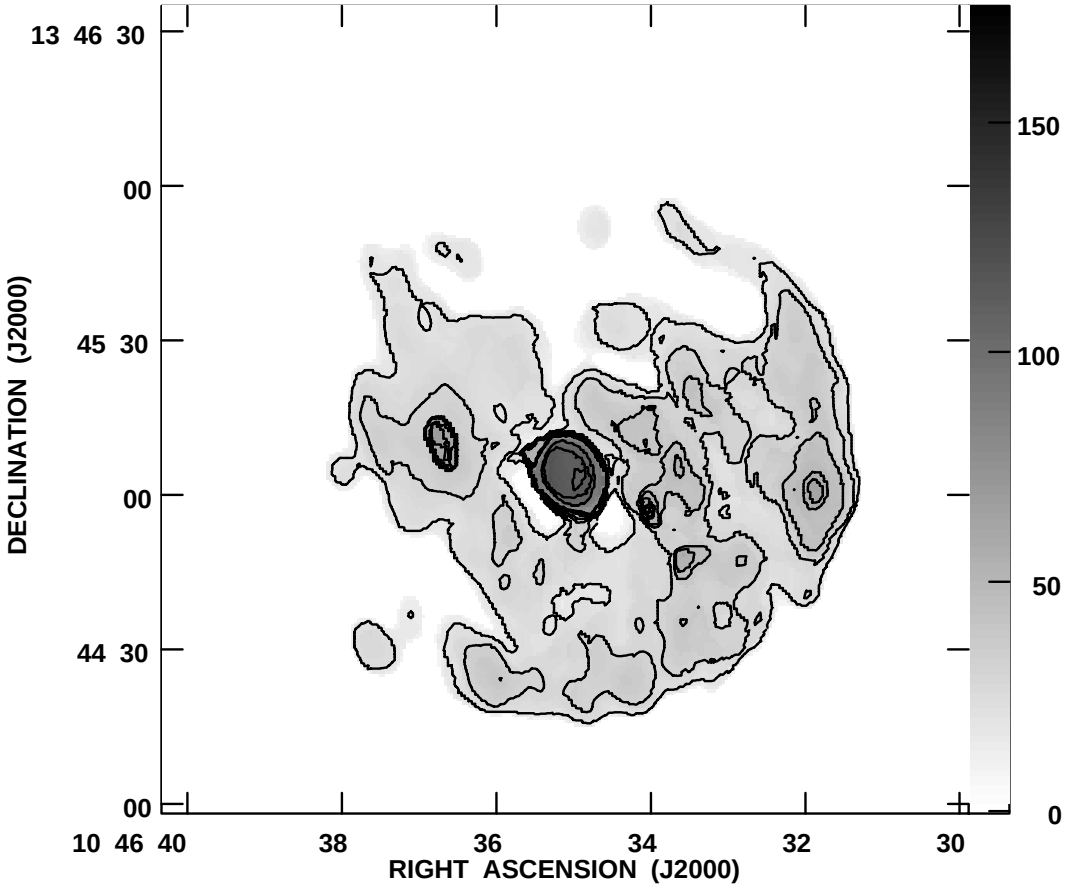


FIG. 5.—Dispersion velocities (moment 2) map in contours and gray scale. Velocity contours correspond to 20, 30, 40, 50, 60, 65, 70, 100, and 110 km s^{-1}.

TABLE 1

INCLINATION OF NGC 3367 WITH RESPECT TO THE PLANE OF THE SKY

i (deg)	Method[a]	References
37.....	Axial ratio and spiral structure	1
32.....	Axial ratio (RC2)	2
0.....	Axial ratio (UGC)	3
17.....	Axial ratio (UGC)	4
25.....	Fits to H I spectra	5
25.....	Axial ratio (RC2)	6
24.....	Axial ratio (RC2)	7
6.....	Fits to optical brightness distribution	8
19.....	Axial ratio (UGC)	9
30.....	Axial ratio (RC3)	10
30.....	Axial ratio (RC3)	11[b]
30.....	Fabry-Pérot Hα	12

[a] RC2: Second Reference Catalog of Bright Galaxies (de Vaucouleurs, de Vaucouleurs, & Corwin 1976); RC3: Third Reference Catalog of Bright Galaxies (de Vaucouleurs et al. 1991); UGC: Uppsala General Catalog of Galaxies (Nilson 1973).

[b] Ho et al. 1997 report in their Table 11, col. (10) values of inclination of disk to the line of sight; however, we believe that they probably meant inclination to the plane of the sky.

REFERENCES.—(1) Danver 1942; (2) de Vaucouleurs et al. 1976; (3) Nilson 1973; (4) Williams & Kerr 1981; (5) Helou et al. 1981; (6) Bottinelli, Gouguenheim, & Paturel 1982; (7) Huchtmeier & Seiradakis 1985; (8) Grösbol 1985; (9) Tully 1988; (10) de Vaucouleurs et al. 1991; (11) Ho et al. 1997; (12) this work.

tance where optical Hα emission was detected) and a model to account for nonzero vertical or radial components are a must in order to make a detailed modeling of the mass distribution (bulge, disk, and halo; see, e.g., Kent 1987; van der Kruit 1990; Freeman 1992; Olling 1996; Sicotte & Carignan 1997; Ryder et al. 1998).

Finally, we obtained the following values for NGC 3367, based on our Fabry-Pérot observations:

1. Center at $\alpha = 10^{h}46^{m}35\overset{s}{.}06$, $\delta = +13°45'04\overset{''}{.}1$ (J2000.0);
2. Position angle of receding major axis, P.A. $= 51° \pm 3°$;
3. Inclination with respect to plane of sky, $i = 30^{+2}_{-5}$ deg;
4. Systemic velocity, $V_{sys} = 3032 \pm 3$ km s^{-1};
5. Maximum rotation velocity, $V_{max} = 210 \pm 15$ km s^{-1};
6. Radius at maximum velocity, $R_{max} = 52'' \pm 3''$; and
7. Dynamical mass inside 52″, $M_{dyn} = 2^{+0.5}_{-0.25} \times 10^{11}$ $M_{\odot}$.

5. DISCUSSION

NGC 3367 is known to exhibit two large ($\approx$2 kpc diameter) radio continuum lobes straddling the nucleus at a distance of about 6 kpc (García-Barreto et al. 1998), while at high resolution, there is a compact nuclear source ($\leq$70 pc in diameter) surrounded by a structure at a radius of less than 350 pc (García-Barreto & Rudnick 2001), with prob-

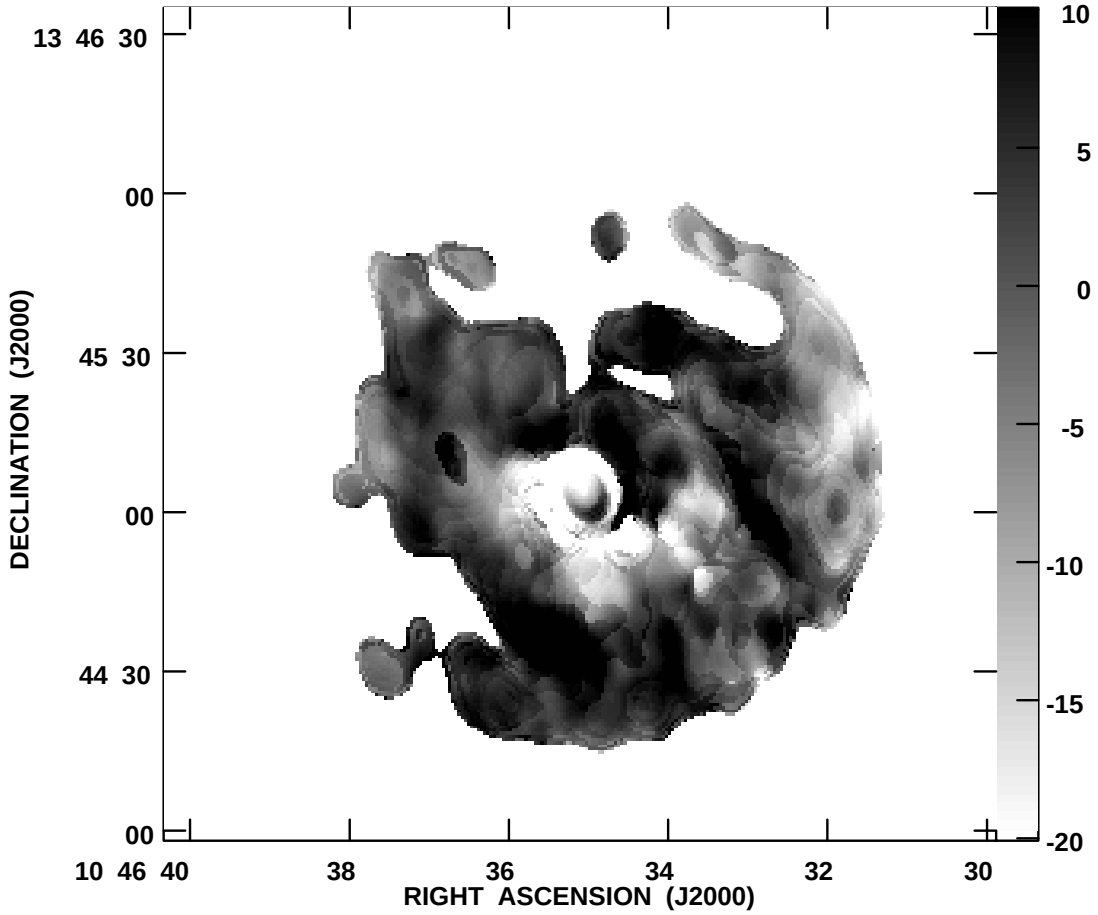


FIG. 6.—Residual velocities (observed minus model) map in gray scale. Scale shown corresponds to -20 up to $+10$ km s^{-1}. Note (1) a velocity asymmetry in the central region at a position angle (P.A. at about 18°) compared with the P.A. of the disk at about 51°, possibly suggesting a different inclination from the central region; and (2) the negative residual velocities mainly from the southwestern semicircle structure. This map was used in order to get the minimum residual velocities and asymmetries, when fitting for the position angle of the semimajor axis and the inclination of the galaxy.

able presence of W-R stars from optical spectroscopy (Ho et al. 1995). Hα optical imaging observations, show an unresolved bright source, most likely associated with the compact nucleus and weak extended emission, covering the innermost 5″, but the existence of a possible circumnuclear structure is difficult to confirm because of poor angular resolution (García-Barreto et al. 1996a, 1996b). Our Fabry-Pérot observations were not the exception, since we also had a very low final angular resolution, as mentioned earlier. Spectra from NGC 3367 in the red optical region indicates a moderate width of the Hα line only to be considered to have an H II nucleus (Ho et al. 1997). Only 2 out of 10 SBc galaxies from the list observed by Martin (1995) have bars with semiaxes smaller than the bar in NGC 3367, suggesting that the bar in NGC 3367 is small, given its Hubble type. From high-resolution radio continuum observations, the lobes are connected to the central region, but this emission is most likely also out of the plane and not

TABLE 2

PARAMETERS OF ROTATION CURVE OF THE GALAXY NGC 3367 IN THIS WORK

i (deg)	P.A. (deg)	V_{sys} (km s^{-1})	V_{max} (km s^{-1})	R_{max} (arcsec)	Parameter Fixed
30.....	52	3034	208	49	None
27.....	49	3028	241	37	x, y, i receding only
27.....	53	3037	291	230	x, y, i approaching only
27.....	52	3032	227	48	x, y, i both sides
31.....	51	3032	199	46	x, y, P.A. both sides
20.....	51	3032	302	55	x, y, P.A., i both sides
30.....	51	3032	204	48	x, y, P.A., V_{sys} both sides
25.....	46	3032	244	49	x, y, P.A., V_{sys} both sides
29.....	53	3032	213	51	x, y, V_{sys} both sides $R_i = 5''$, $R_o = 75''$
30.....	51	3032	211	38	x, y, P.A., V_{sys} receding side only $\pm 60°$ from P.A.
30.....	51	3032	253	185	x, y, P.A., V_{sys} approaching side only $\pm 60°$ from P.A.
30.....	51	3032	210	52	x, y, P.A., i, V_{sys} both sides only

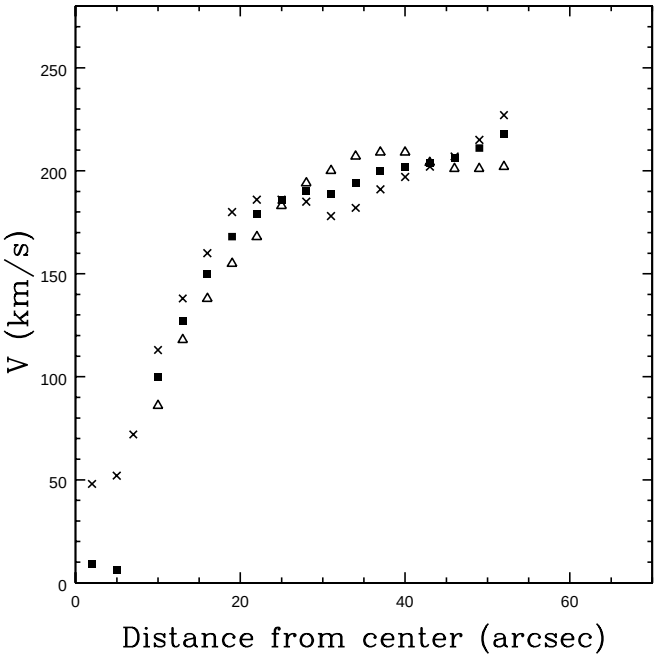


FIG. 7.—Final rotation curve for NGC 3367 determined from Fabry-Pérot observations using the receding side only (*open triangles*), the approaching side only (*crosses*), and both the receding and approaching sides (*filled squares*). Error uncertainties in velocity vary from 2 to 15 km s^{-1}. Here 1″ corresponds to 210 pc.

associated with any dust or shock regions along the stellar bar, since these are expected to be on the leading side of the bar, southeast and northwest, assuming that the bar is rotating counterclockwise as suggested by the trailing arms (as seen in other galaxies, e.g., NGC 1365; Jörsater & van Moorsel 1995). The presence of radio continuum lobes out from the nuclear region and X-ray emission indicates the presence of activity and suggests an inflow process to the very center of the galaxy. The high-dispersion velocity found in the central region (of up to 120 km s^{-1}) might be associated with the circumnuclear structure and probable outflow (since emission is observed at different velocity channels; see Fig. 3). Starburst-driven galaxy outflows have been reported for several strong far-infrared emitters (Heckman, Armus, & Miley 1990). Faint broad optical emission lines have been modeled as being associated with shells of interstellar material smoothly accelerated after breakout (Tenorio-Tagle et al. 1997). The existence of an unresolved radio continuum source ($\leq$70 pc in diameter) hints that the source of energy is a compact nucleus; however, optical spectroscopy fails to detect emission from high-ionization atoms (i.e., Fe) in NGC 3367 as is detected from other active galactic nuclei (Ho, Filippenko, & Sargent 1995). The source of the central activity is still to be resolved and is beyond the scope of the present work. Since the raw rotation curve in Figure 7 most likely includes nonzero vertical and radial components of the velocity at different radii, the derived angular velocity is therefore ambiguous, as are the radial frequencies [(since $\kappa(R)$ depends on Ω and $d\Omega/dR$)]. However, if the southwestern ring were the result of an outer Lindblad resonance at a distance between 8.5 and 10 kpc, a possibility that was discarded because of the lack of symmetry on the northeastern side (García-Barreto et al. 1996a), then the estimated constant angular velocity of the bar would be close to 43 km s^{-1} kpc^{-1}, and the corotation (CR) would be at a radius between 3.5 and 4 kpc, which would correspond to about 1 and 1.25 times the radius of the stellar bar. These estimates must clearly be taken with caution and only as a zero order, but it is fair to say that they are in agreement with values given for other barred galaxies (Buta & Combes 1996). However, nothing could be said about the distance from the nucleus expected for an inner Lindblad resonance (ILR), which in general for Sc galaxies is expected to be at larger radii than for Sa galaxies simply as a result of mass concentration in early-type galaxies. For the structure in high-resolution radio continuum observations between 0.3 and 0.45 kpc from the compact nucleus, it remains to be proven whether it lies near an ILR.

Deviations from circular orbits have been routinely observed in almost every spiral galaxy (Teuben et al. 1986; Giovanelli & Haynes 1988; Rots et al. 1990; Jörsater & van Moorsel 1995; Sicotte & Carignan 1997; Beauvais & Bothun 1999). Substantial noncircular streaming motions and large residual velocities were found in the inner bar region of NGC 1365 (Teuben et al. 1986; Jörsater & van Moorsel 1995). In the case of NGC 3367, isovelocity contours from (1) the central region and (2) southwestern (approaching side) outermost regions of the galaxy are observed to deviate from normal circular motion. For example, the isovelocity contours from the south in NGC 3367 indicate an observed bluer velocity of about 20 to 30 km s^{-1}, at a radius of about 8.5 kpc from the nucleus, than the expected value; a similar behavior is observed from the western bright sources (see Fig. 4). In particular, from inspection of the channel velocity maps (Fig. 3), the western bright region shows from the first channel at 2898 km s^{-1} up to the channel at velocity 3031 km s^{-1}, suggesting an expanding bubble of about 65 km s^{-1}, centered at a radial velocity of 2965 km s^{-1}, which would correspond to the expected circular velocity. The central and bright eastern regions show up in different velocity channels, possibly suggesting the existence of expanding gas also; however, more detailed observations are needed in order to confirm this idea.

Large velocity dispersions from the central region in NGC 3367 might be associated with an outflow. Reasons in favor are as follows: (1) a plasma outflow is definitely there, since NGC 3367 presents two radio continuum lobes connected to the nucleus at a radii of 6 kpc; (2) a probable circumnuclear structure (García-Barreto & Rudnick 2001) with W-R stars (Ho et al. 1995); and (3) X-ray emission (Giogia et al. 1990).

A possible interpretation for large velocity dispersions from the southwestern semiring (see Fig. 4) might be that these sources are part of a structure with a higher radial velocity, from 10 to 40 km s^{-1}, than expected at their radii, assuming circular orbits (Beauvais & Bothun 1999). This radial velocity could be the result of the coeval evolution of H II regions in a normal disk, or it could be the result of a large-scale phenomenon (i.e., bow shock [Kritsuk 1983], outward wave [Lynds & Toomre 1976; Toomre 1978]; etc.). Yet, another possibility is that the semiring of Hα sources is at a higher inclination with respect to the plane of the sky and, therefore, inclined with respect to the galaxy interior disk. If the outer region were a warp (Binney 1992), it would show up in atomic hydrogen observations.

Finally, Grösbol (1985) has studied the mass distribution of many spiral galaxies from azimuthal intensity profiles based on POSS red plates, including NGC 3367. Values

found by him are as follows: a radius with a mean surface brightness of 23.5 mag arcsec^{-2}, $r_{23.5} = 74''$; an inner radius in which the mean intensity could be approximated by an exponential disk, $r_i = 6''$; an outer radius in which the mean intensity could be approximated by an exponential disk, $r_o = 46''$; and a scale length of the exponential disk, $r_l = 24''.3$. Baggett, Baggett, & Anderson (1998) also have reported a bulge-disk decomposition for 659 spiral galaxies, including NGC 3367, based on major-axis brightness profiles from the Photometric Atlas of Northern Bright Galaxies by Kodaira, Okamura, & Ichikawa (1990). They fitted de Vaucouleurs' law profiles for bulges and a truncated exponential disk (after Kormendy). For NGC 3367, in particular, they report a disk scale length of 8″, a disk truncation radius of 26″.6, and a bulge effective radius of 25″.8. It is pertinent here to repeat that NGC 3367 has a stellar bar in a P.A. = 63° ± 5° and a radius of only 16″ (García-Barreto et al. 1996a, 1996b), and thus the bulge-disk decomposition by Baggett at al. includes the stellar bar inside what they consider a bulge. A detailed model of the mass distribution in NGC 3367, including bulge, disk, and halo, is necessary, and it would benefit from not only optical surface photometry and velocity field, but also from extended atomic hydrogen gas and velocity distributions.

6. CONCLUSIONS

We have carried out Fabry-Pérot Hα emission observations from the barred galaxy NGC 3367 field with the PUMA equipment at the San Pedro Mártir 2.12 m telescope in order to determine the velocity field in NGC 3367. Important results can be summarized as follows: (1) We have determined the values for different parameters. The inclination of the disk with respect to the plane of the sky is $i = 30°$; the position angle of the receding semimajor axis is P.A. = 51°; the systemic velocity is $V_{sys} = 3032$ km s^{-1}; the maximum rotation velocity is $V_{max} = 210$ km s^{-1}; and the radius at which maximum rotation velocity is attained is $R_{max} = 52''$ (10.9 kpc). (2) We estimated a dynamical mass inside 52″ to be $M_{dyn} = 2 \times 10^{11}\ M_\odot$, based on the maximum rotation velocity. (3) We have detected large velocity dispersions (up to 120 km s^{-1}) in the central region, from the bright regions in the west at about 10 kpc from the nucleus (with velocities up to 60 km s^{-1}), and from the bright regions just east of the end of the stellar bar (with velocities up to 70 km s^{-1}). The velocity dispersion from the central region might be associated with the presence of an outflow from either a compact nucleus or a circumnuclear structure and regions of intense star formation with W-R stars. (4) We observed deviations from the isovelocity contours from the southwestern (approaching side) outermost regions of the galaxy, coinciding with the string of bright Hα sources. A possible interpretation is that these sources are part of a semiring with a higher radial velocity, from 10 to 40 km s^{-1}, than expected at their radii, assuming circular orbits, or that this region is at different inclination than the plane of the galaxy.

We would like to thank the anonymous referee for useful comments and suggestions on how to improve the paper. We acknowledge fruitful conversations with E. Moreno and V. Avila-Reese. M. Rosado acknowledges partial financial support from CONACYT (México) grant 27984-E and from DGAPA. (UNAM, México) grant IN122298.

REFERENCES

Aaronson, M., Mould, J., & Huchra J. 1980, ApJ, 237, 655
Baggett, W. E., Baggett, S. M., & Anderson, K. S. J. 1998, AJ, 116, 1626
Beauvais, C., & Bothun, G. 1999, ApJS, 125, 99
Binney, J. 1992, ARA&A, 30, 51
Bosma, A. 1981, AJ, 86, 1791
Bottinelli, L., Gouguenheim, L., & Paturel, G. 1982, A&A, 113, 61
Brandt, J. C. 1960, ApJ, 131, 293
Buta, R., & Combes, F. 1996, Fundam. Cosmic Phys., 17, 95
Danver, C. G. 1942, Lunds Obs. Ann, No. 10
de Vaucouleurs, G., de Vaucouleurs, A., & Corwin, H. G., Jr. 1976, Second Reference Catalog of Bright Galaxies (Austin: Univ. of Texas Press)
de Vaucouleurs, G., de Vaucouleurs, A., Corwin, H. G., Jr., & Buta, R. 1991, Third Reference Catalog of Bright Galaxies (New York: Springer)
Freeman, K. C. 1992, in Physics of Nearby Galaxies: Nature or Nurture?, ed. R. X. Thuan, C. Balkowski, & J. T. Thanh Van (Gif-sur-Yvette: Edition Frontières), 201
García-Barreto, J. A., Franco, J., & Carrillo, R. 1996a, ApJ, 469, 138
García-Barreto, J. A., Franco, J., Carrillo, R., Venegas, S., & Escalante-Ramirez, B. 1996b, Rev. Mexicana Astron. Astrofis., 32, 89
García-Barreto, J. A., & Rudnick, L. 2001, in preparation
García-Barreto, J. A., Rudnick, L., Franco, J., & Martos, M. 1998, AJ, 116, 111
Gioia, I. M., Maccacaro, T., Schild, R. E., Wolter, A., Stocke, J. T., Morris, S. L., & Henry, J. P. 1990, ApJS, 72, 567
Giovanelli, R., & Haynes, M. P. 1988, in Galactic and Extragalactic Radio Astronomy, ed. G. L. Verschuur & K. I. Kellerman (2d ed.; New York: Springer Verlag), 522
Grösbol, P. J. 1985, A&AS, 60, 261
Heckman, T. M., Armus, L., & Miley, G. K. 1990, ApJS, 74, 833
Helou, G., Goivanardi, C., Salpeter, E. E., & Krumm, N. 1981, ApJS, 46, 267
Ho, L. C., Filippenko, A. V., & Sargent, W. L. W. 1995, ApJS, 98, 477
———. 1997, ApJS, 112, 315
Holmberg, E. 1958, Medd. Lunds Astron. Obs. Ser. 2, 136, 1
Hubble, E. 1926, ApJ, 64, 321
Huchtmeier, W. K., & Seiradakis, J. H. 1985, A&A, 143, 216
Jörsater, S., & van Moorsel, G. A. 1995, AJ, 110, 2037
Kent, S. M. 1987, AJ, 93, 816
Kodaira, K., Okamura, S., & Ichikawa, S., ed. 1990, Photometric Atlas of Northern Bright Galaxies (Tokyo: Univ. Tokyo Press)
Kritsuk, A. G. 1983, Astrofizika, 19, 471
Le Coarer, E., Rosado, M., Georgelin, Y., Viale, A., & Goldes, G. 1993, A&A, 280, 365
Lynds, R., & Toomre, A. 1976, ApJ, 209, 382
Martin, P. 1995, AJ, 109, 2428
Mirabel, I. F., & Sanders, D. B. 1988, ApJ, 335, 104
Mihalas, D., & Binney, J. 1981, Galactic Astronomy (2d ed.; San Francisco: Freeman)
Nilson, P. 1973, Uppsala General Catalog of Galaxies (Uppsala: Uppsala Astr. Obs.)
Olling, R. P. 1996, AJ, 112, 457
Rosado, M., et al. 1995, in The Fifth Mexico-Texas Conference on Astrophysics, ed. M. Peña & S. Kurtz (Rev. Mexicana Astron. Astrofis. Ser. Conf. 3) (México, D. F.: Inst. Astron., Univ. Nac. Autónoma de México), 263
Rots, A. H., Bosma, A., van der Hulst, J. M., Athanassoula, E., & Crane, P. C. 1990, AJ, 100, 387
Rubin, V. C., Burstein, D., Ford, W. K., Jr., & Thonnard, N. 1985, ApJ, 289, 81
Rubin, V. C., Waterman, A. H., & Kenney, J. D. P. 1999, AJ, 118, 236
Ryder, S. D., Zasov, A. V., McIntyre, V. J., Walsh, W., & Sil'chenko, O. K. 1998, MNRAS, 293, 411
Sicotte, V., & Carignan, C. 1997, AJ, 113, 609
Staveley-Smith, L., & Davies, R. D. 1988, MNRAS, 231, 833
Tenorio-Tagle, G., Muñoz-Tuñón, C., Pérez, E., & Melnick, J. 1997, ApJ, 490, L179
Teuben, P., Sanders, R. H., Atherton, P., & van Albada, G. 1986, MNRAS, 221, 1
Toomre, A. 1978, in IAU Symp. 79, The Large Scale Structure of the Universe, ed. M. S. Longair & J. Einasto (Dordrecht: Reidel), 109
Tully, R. B. 1988, in Nearby Galaxy Catalog (Cambridge: Cambridge Univ. Press)
van der Kruit, P. C. 1990, in The Milky Way as a Galaxy, ed. R. Buser & I. R. King (Mill Valley: University Science Books), 185
van Moorsel, G. A., & Wells, D. C. 1985, AJ, 90, 1038
Véron-Cetty, M.-P., & Véron, P. 1986, A&AS, 66, 335
Véron, P., Gonçalves, A. C., & Véron-Cetty, M.-P. 1997, A&A, 319, 52
Williams, B. A., & Kerr, F. J. 1981, AJ, 86, 953